SUPPLEMENT

Molecular modeling of apoE in complexes with Alzheimer's amyloid-β fibrils from human brain suggests a structural basis for apolipoprotein co-deposition with amyloids

Emily Lewkowicz, Mari N. Nakamura, Michael J. Rynkiewicz, Olga Gursky

CONTENT:

Supplemental Figures 1-9, Supplemental Table 1

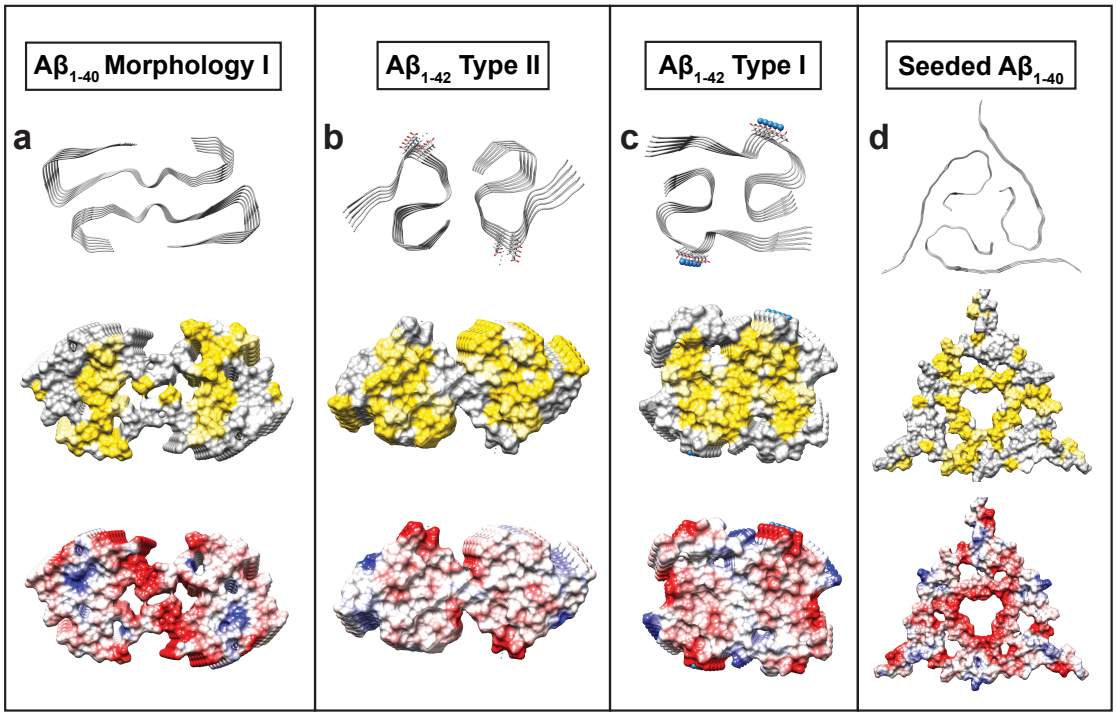

Supplemental Fig. 1 Structural polymorphs of patient-based $A\beta_{1-40}$ and $A\beta_{1-42}$ fibrils used in the current study. Views down the fibril axis show ribbon diagrams (top) and space-filling models depicting hydrophobic (middle) and Coulombic surfaces (bottom). Color coding in these and in other space-filling models: hydrophobic – yellow, acidic – red, basic – blue.

(**a**) $A\beta_{1-40}$ fibril morphology I from AD vasculature, cryo-EM structure (PDB ID: 6SHS);
(**b**) $A\beta_{1-42}$ type II from parenchymal deposits, cryo-EM structure (PDB ID: 7Q4M);
(**c**) $A\beta_{1-42}$ type I from parenchymal deposits, cryo-EM structure (PDB ID: 7Q4B);
(**d**) $A\beta_{1-40}$ seeded fibril with seed isolated from AD brain tissue, NMR structure (PDB ID: 2M4J).

In panels b and c, small blue spheres indicate putative metal ions bound *via* acidic ladders of E22, D23.

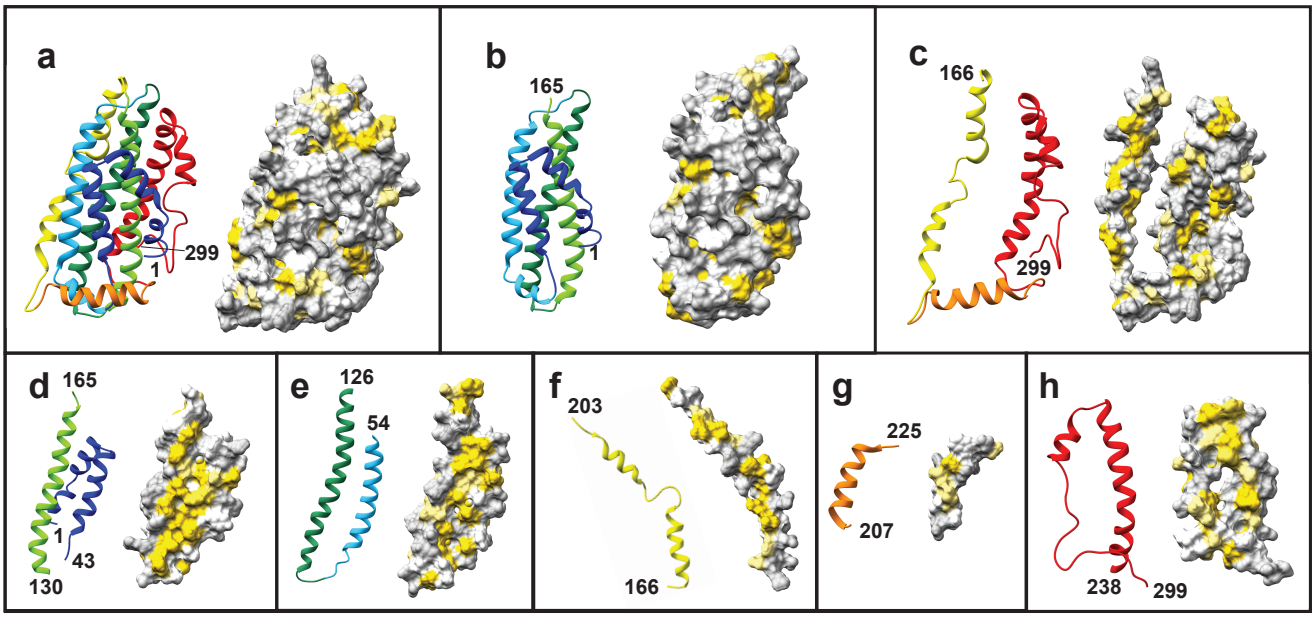

Supplemental Fig. 2 Solution NMR structure of full-length lipid-free modified human apoE3 (PDB ID: 2L7B) and its fragments used in the current study. Helices in the ribbon diagrams are rainbow-colored N to C (blue to red). Space-filling models are oriented to show hydrophobic surfaces (in yellow). First and last residues in each fragment are shown by numbers.
(**a**) Full-length apoE; (**b**) NTD; (**c**) CTD. (**d-h**) Segments that yielded consistent results in ClusPro docking to amyloid fibrils: (**d**) helices 1 and 4, (**e**) helices 2 and 3, (**f**) hinge, (**g**) lock, and (**h**) CT region.

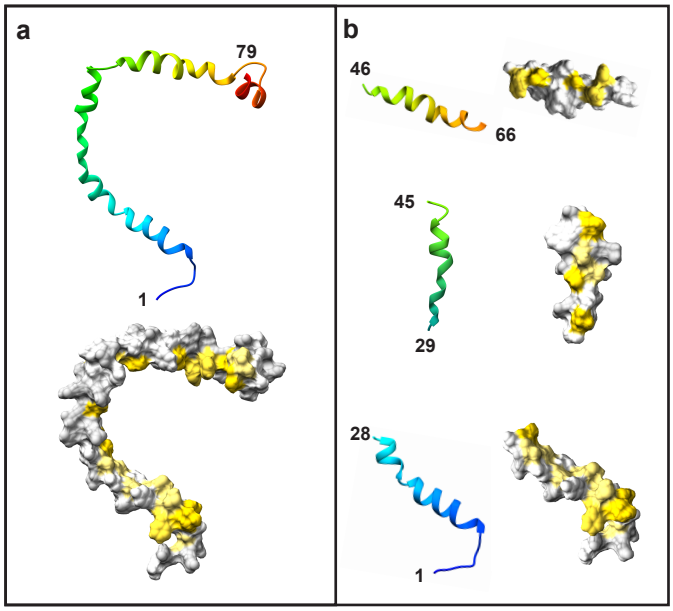

Supplemental Fig. 3 Solution NMR structure of full-length human apoC-III (PDB ID: 2JQ3) and its fragments used in the current study. The structure, which was determined by using the apolipoprotein bound to SDS micelles (diameter ~4.4 nm), represents the lipid-bound conformation. Ribbon diagrams are rainbow colored N to C (blue to red); space-filling models are oriented to show hydrophobic surfaces (in yellow). First and last residue numbers are indicated. (**a**) Full-length apoC-III. (**b**) NT, middle, and truncated CT fragments, which yielded consistent results in ClusPro docking to amyloid fibrils.

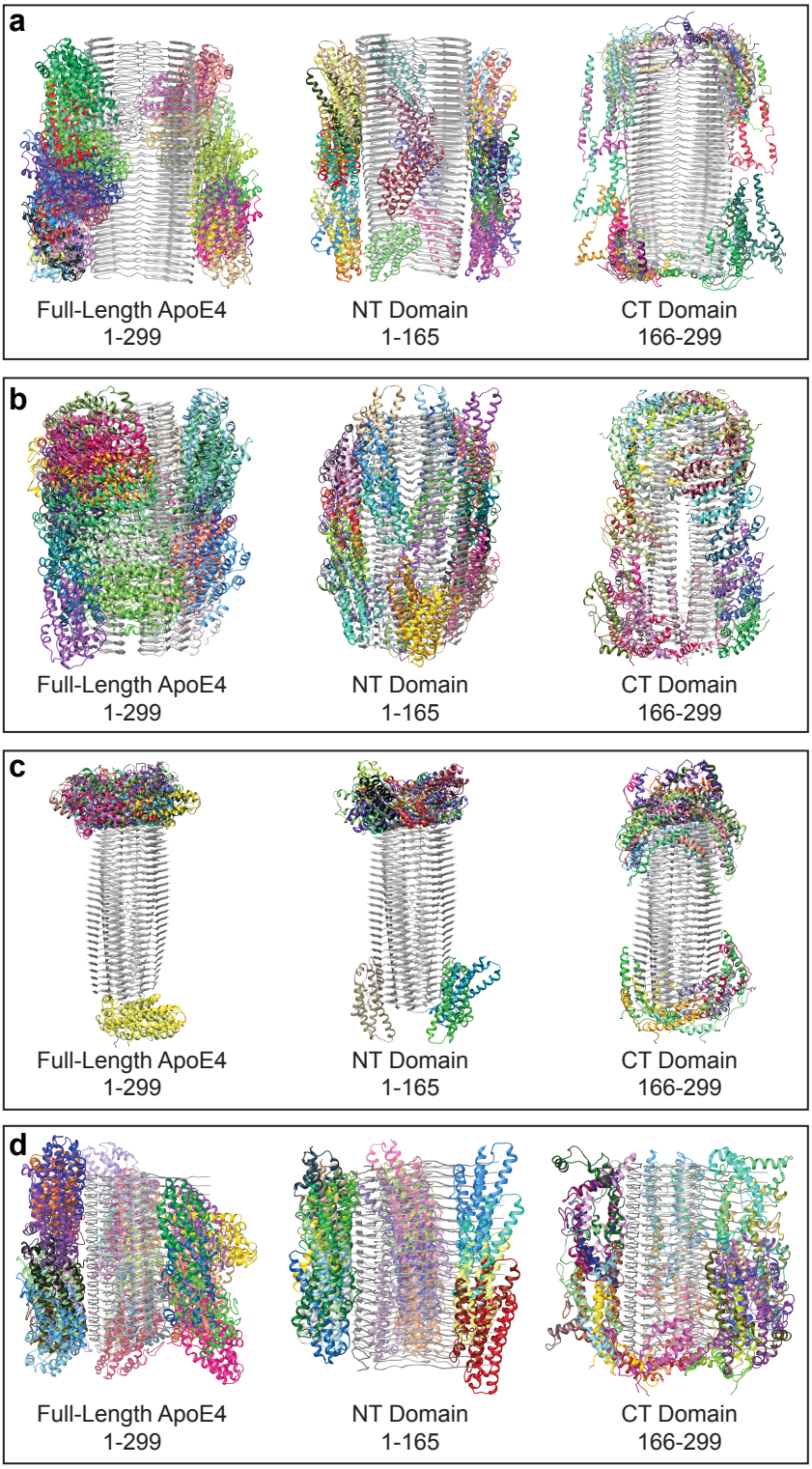

Supplemental Fig. 4 Summary of docking poses for full-length apoE and its NTD and CTD fragments docked using Cluspro onto four Aβ fibrils. Residues in each fragment are shown by numbers. The top-scoring docking poses for each fragment are shown; each pose is colored differently. The fibrils are:
(**a**) $A\beta_{1\text{-}40}$ fibril morphology I from AD vasculature, cryo-EM structure (PDB ID: 6SHS);
(**b**) $A\beta_{1\text{-}42}$ type II from parenchymal deposits, cryo-EM structure (PDB ID: 7Q4M);
(**c**) $A\beta_{1\text{-}42}$ type I from parenchymal deposits, cryo-EM structure (PDB ID: 7Q4B);
(**d**) $A\beta_{1\text{-}40}$ seeded fibril with the seed isolated from AD brain tissue, NMR structure (PDB ID: 2M4J).

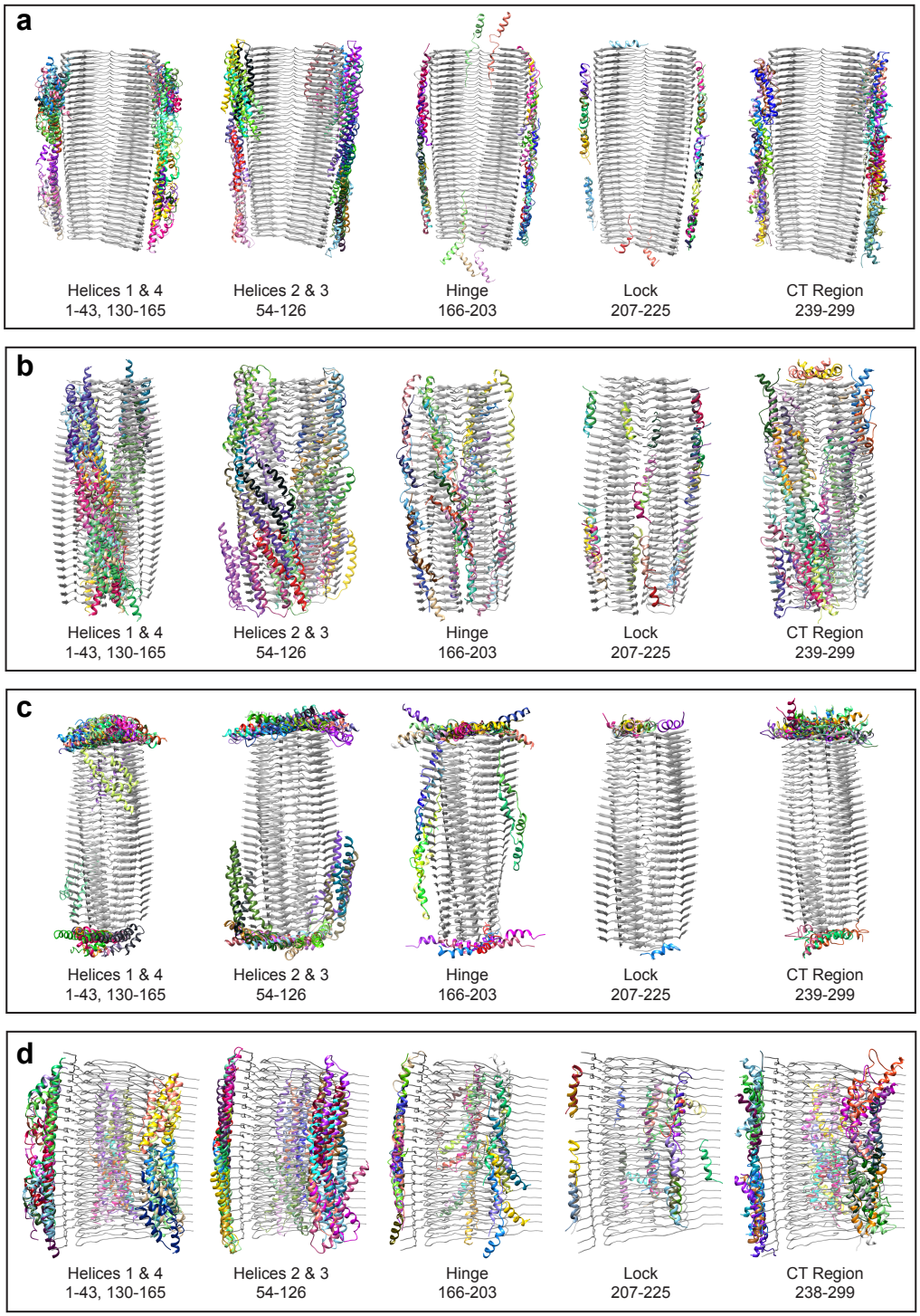

Supplemental Fig. 5 Summary of docking poses for apoE fragments docked onto four different Aβ fibrils. ApoE was split into fragments shown in supplemental Fig. 2d-h; the residues in each fragment are shown by numbers. The top-scoring docking poses for each fragment are shown; each pose is colored differently. The fibril structure is in gray. The fibrils are:
(**a**) $A\beta_{1\text{-}40}$ fibril morphology I from AD vasculature, cryo-EM structure (PDB ID: 6SHS);
(**b**) $A\beta_{1\text{-}42}$ type II from parenchymal deposits, cryo-EM structure (PDB ID: 7Q4M);
(**c**) $A\beta_{1\text{-}42}$ type I from parenchymal deposits, cryo-EM structure (PDB ID: 7Q4B);
(**d**) $A\beta_{1\text{-}40}$ seeded fibril with seed isolated from AD brain tissue, NMR structure (PDB ID: 2M4J)

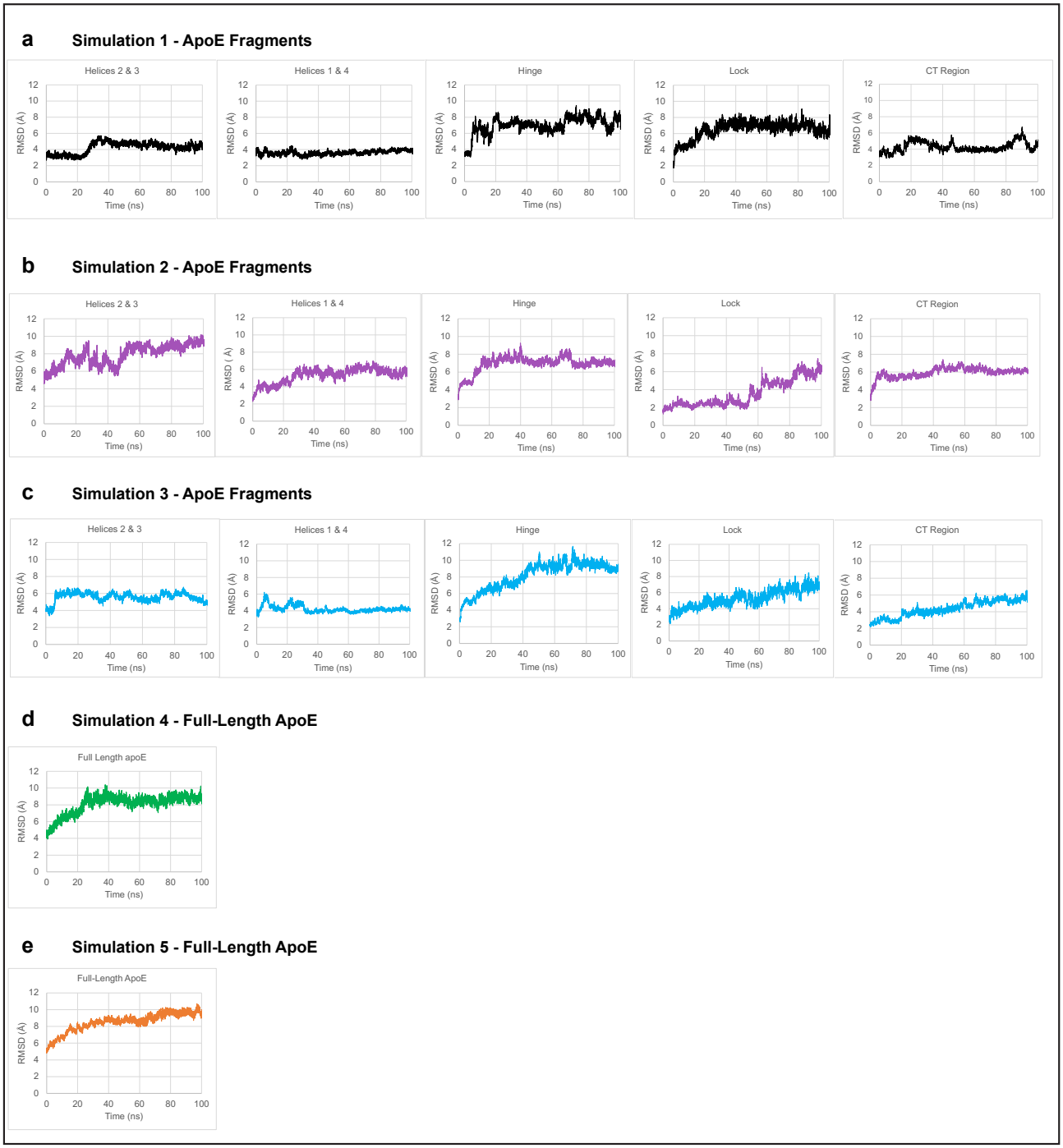

Supplemental Fig. 6 Root mean square deviations (RMSD) for the backbone atoms in MD simulations of apoE in complex with $A\beta_{1\text{-}42}$ type II fibril during production run time. Each model contained either 56 (a, b, d) or 64 fibril rungs (c, e). RMSD are shown for (**a-c**) triplicate simulations of each apoE fragment, and for (**d, e**) duplicate simulations of the full-length apoE model generated from these fragments as described in the text. For RMSD measurements, each frame was aligned by C_α atoms either by fibril segments adjacent to the fragment of interest (in **a-c**) or the entire fibril (in **d-e**).

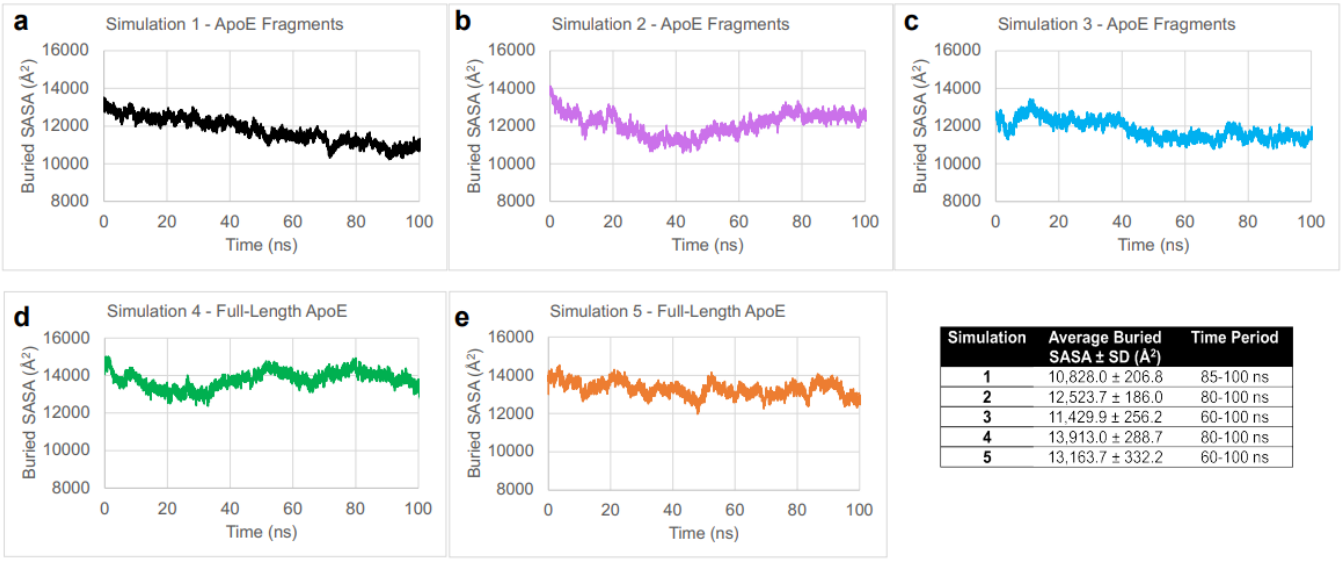

Simulation	Average Buried SASA ± SD (Å²)	Time Period
1	10,828.0 ± 206.8	85-100 ns
2	12,523.7 ± 186.0	80-100 ns
3	11,429.9 ± 256.2	60-100 ns
4	13,913.0 ± 288.7	80-100 ns
5	13,163.7 ± 332.2	60-100 ns

Supplemental Fig. 7 Buried solvent-accessible surface area (SASA) between apoE and $A\beta_{1-42}$ fibril during MD simulations. The values are shown for (**a-c**) triplicate simulations of apoE fragments in complex with $A\beta_{1-42}$ type II fibril, and for (**d, e**) duplicate simulations of the full-length apoE – fibril model generated from these fragments. Respective models are shown in Fig 2b, d of the main manuscript. Average buried SASA for the last 20-40 ns of the production run is tabulated for each simulation.

Aβ	***ApoE***
Glu22	Lys143
Asp23	Lys95, Gln98, Arg136, Ser139, Arg142, Lys143, Lys146, Arg147, Arg150, Arg158, Arg217, Met221, Arg224, Arg274, Gln279, Gln284, Thr289, Ser290
Val24	Arg147, Met221, Arg224, Gln284, Thr289, Ser290
Gly25	His140, Arg147, Met218, Met221, Arg224, Gln284, Ala285, Thr289, Ser290
Ser26	His140, Met218
Val36	Arg25, Leu28, Tyr36, Trp39, Gln81, Arg167
Gly37	Arg25, Leu28, Ala29, Tyr36, Trp39, Leu63, Gln81, Arg167, Glu168
Gly38	Arg25, Trp26, Leu28, Ala29, Tyr36, Trp39, Val56, Leu60, Leu63, Tyr74, Gln81, Glu168, Gly169
Val39	Trp26, Ala29, Leu30, Phe33, Tyr36, Leu27, Trp39, Val40, Leu60, Leu63, Met64, Thr67, Leu71, Tyr74, Leu78, Thr83, Glu87, Glu88, Leu104, Met108, Val111, Tyr118, Met125, Leu133, Leu137, Leu159, Tyr162, Gln163, Gly169, Arg172, Gly173, Ala176, Ile177, Leu198, Ala199, Arg215, Ile250, Arg251, Gln253, Ala254, Ala257, Phe265, Val294, Pro295
Ile41	Ala91, Arg92, Arg103, Val111, Arg114, Met125, Leu133, Leu137, His140, Leu141, Asp151, Leu155, Leu159, Tyr162, Arg172, Ala176, Arg180, Leu181, Gln187, Arg189, Val190, Ala193, Leu198, Ala199, Trp210, Gly211, Leu214, Arg215, Met218, Glu219, Gly222, Ser223, Ile250, Phe265, Ala269, Gln273, Trp276, Ala292

Supplemental Table 1. Contact table listing close contacts between the backbone atoms of amino acids from apoE and $A\beta_{1-42}$ fibrils from parenchymal deposits of AD patients. Contacts within 5Å which are seen in ≥75% of frames are listed for simulation 3 of the model containing apoE fragments and $A\beta_{1-42}$ type II fibril. The model, which is shown in Fig. 2b of the main manuscript, was subjected to MD simulations as described in the text. Representative simulation 3 was used to determine the contacts; RMSD and buried SASA for simulation 3 are shown in supplemental Figs. 6c and 7c.

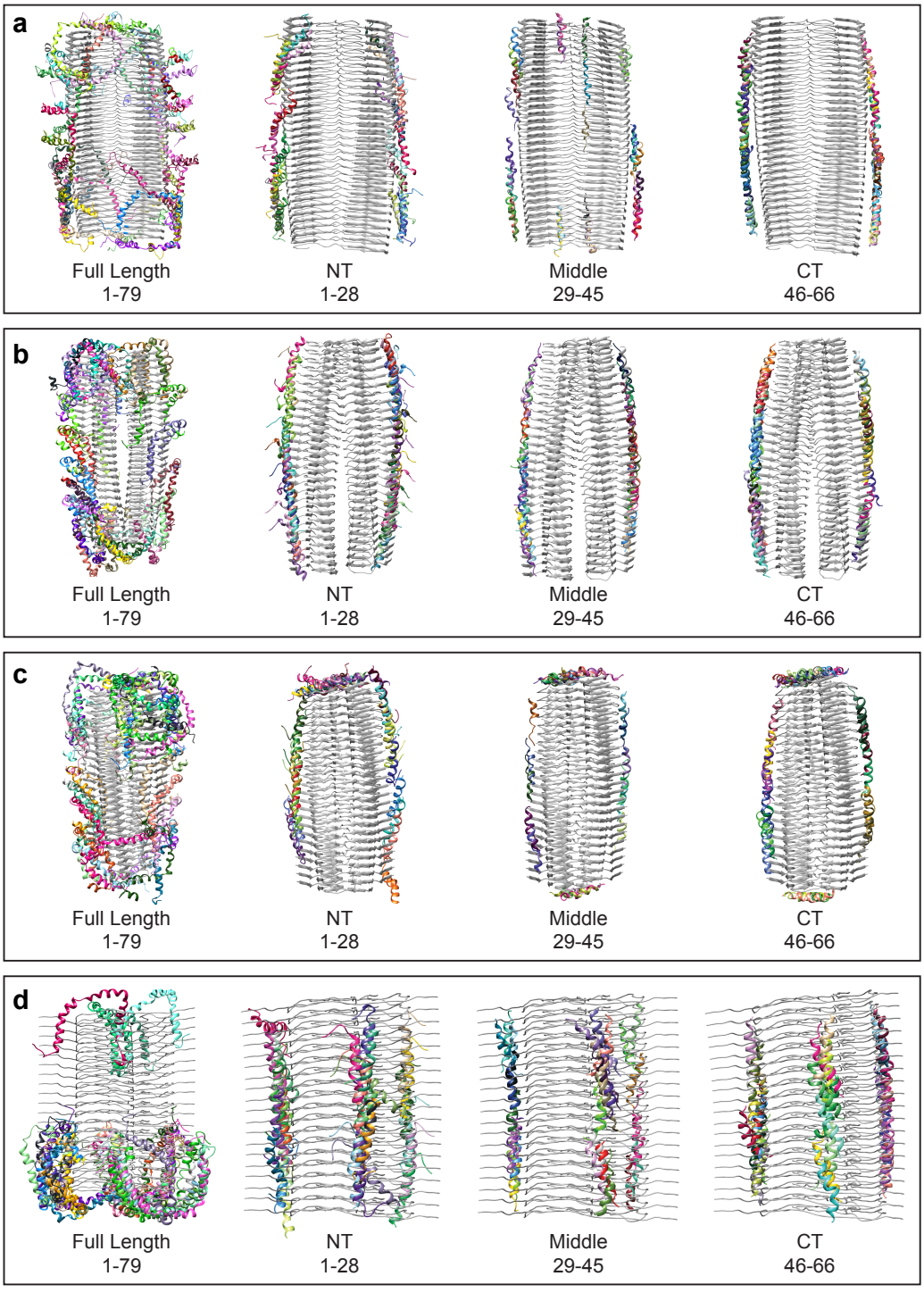

Supplemental Fig. 8 Summary of docking poses for full-length apoC-III and its NT, middle, and truncated CT fragments docked onto four different Aβ fibrils. Residues numbers in each protein fragment are shown. Top-scoring docking poses are shown, each is colored differently. The fibrils are:
(**a**) $A\beta_{1\text{-}40}$ fibril morphology I from AD vasculature, cryo-EM structure (PDB ID: 6SHS);
(**b**) $A\beta_{1\text{-}42}$ type II from parenchymal deposits, cryo-EM structure (PDB ID: 7Q4M);
(**c**) $A\beta_{1\text{-}42}$ type I from parenchymal deposits, cryo-EM structure (PDB ID: 7Q4B);
(**b**) $A\beta_{1\text{-}40}$ seeded fibril with seed isolated from AD brain tissue, NMR structure (PDB ID: 2M4J).

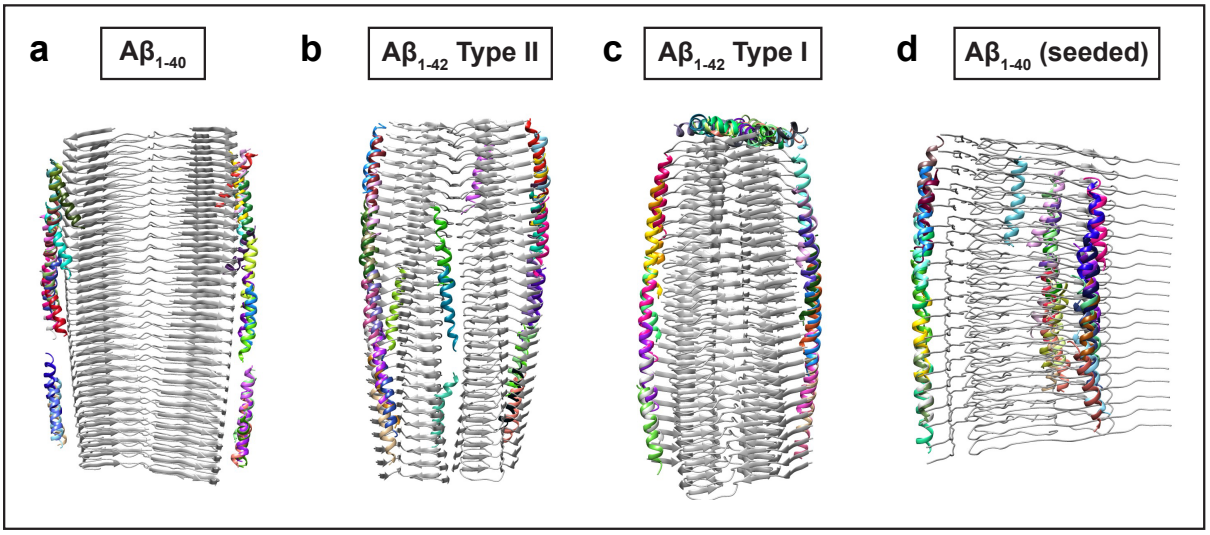

Supplemental Fig. 9 Summary of docking poses for the consensus sequence peptide to Aβ fibrils. CSP, which is comprised of a 22-residue sequence repeat motif representing class-A amphipathic α-helices found in apoA-I, apoA-IV and apoE (PLAEELRARLRAQLEELRERLG), was docked onto four different Aβ fibrils. Top-scoring docking poses are shown; each is colored differently. The fibrils are:
(**a**) $A\beta_{1\text{-}40}$ fibril morphology I from AD vasculature, cryo-EM structure (PDB ID: 6SHS);
(**b**) $A\beta_{1\text{-}42}$ type II from parenchymal deposits, cryo-EM structure (PDB ID: 7Q4M);
(**c**) $A\beta_{1\text{-}42}$ type I from parenchymal deposits, cryo-EM structure (PDB ID: 7Q4B);
(**b**) $A\beta_{1\text{-}40}$ seeded fibril with seed isolated from AD brain tissue, NMR structure (PDB ID: 2M4J).